

Picometer metrology for precise measurement of refractive index, pressure, and temperature

Speaker: Jack Stone, National Institute of Standards and Technology, 100 Bureau Dr. stop 8211, Gaithersburg, MD, 20899-8211, 301-975-5638, jack.stone@nist.gov

Authors: P. Egan, J. Hendricks, G. Strouse, D. Olson, J. Ricker, G. Scace, National Institute of Standards and Technology

Abstract: For several years we have been studying the use of Fabry-Perot interferometers for precise measurement of the refractive index of gasses, where the primary motivation has been to improve interferometer-based length measurement. Because the refractive index of a gas depends on its pressure and temperature, we can also use refractive index to monitor either of these quantities if the second is known. Recently we have embarked on a project that will utilize refractive index to infer pressure with a smaller measurement uncertainty than is currently possible, hoping to reach a relative standard uncertainty of 1.4×10^{-6} . The projected uncertainty budget is currently dominated by uncertainty of the Boltzmann constant, but following the coming redefinition of SI units, the Boltzmann uncertainty will be replaced by uncertainty in the temperature scale, at which point refractive index measurements can be expected to play a central role in precise realization of thermodynamic temperature.

Dimensional metrology with picometer uncertainties is the core of our technique and is the subject of this paper. Refractive index will be measured by comparing two precisely equal displacements (≈ 150 mm), where one displacement is in vacuum and the second is in helium and will appear to be slightly longer due to the refractive index. The two displacements must be compared with < 3 pm uncertainty. The intrinsic precision achievable with Fabry-Perot cavities far exceeds our needed accuracy, but two or more independent interferometers have never been compared to such high accuracy when undergoing macroscopic displacements. The major challenges include many of the typical sources of error in dimensional measurement, such as Abbe errors, alignment errors, material dimensional stability, etc. Careful consideration must be given to second-order effects that are not normally large enough to merit mention. Our proposed experimental design will minimize such errors and provide additional metrology (including angle measurements with nanoradian precision) needed to correct the residual errors.

Learning Objectives: Understanding sources of uncertainty in ultra-high accuracy dimensional measurements.

1. Introduction. We are beginning a project to improve measurement of refractive index of gasses. One motivation is to improve our capability for interferometer-based length measurements in air or other gas environments. A second motivation arises from the fact that refractive index is related to gas density, and consequently this technique can also be used as an indirect measure of either gas pressure or gas temperature if the second quantity is

known/measured. We plan to use this approach as the basis of new pressure and temperature standards. For temperature measurement, the technique is an optical analog of existing methods of gas thermometry based on dielectric constant measurements. For pressure measurements (which is our current focus), the technique holds promise of providing lower uncertainties than presently attainable while eliminating the need for the current mercury-based standards.

The dimensional metrology required to achieve this goal is quite demanding. We need to compare the changes in two optical path lengths, one in vacuum and the other in gas, with an accuracy of a few picometers on an overall displacement of ≈ 15 cm. This article discusses only the dimensional metrology. There are a number of other critical issues involved in inferring pressure (or temperature) from the measurements, but these are beyond the scope of this article.

2. Fixed length Fabry-Perot cavities. For several years we have been using optical cavities to measure refractive index of gasses [1]. Thus far, we have been doing these measurements with Fabry-Perot cavities of fixed length such as shown in Fig. 1. (Variable length cavities will be discussed in the following sections.) Highly reflective mirrors made from low-expansion glass are mounted facing each other, bonded to the ends of a spacer of the same material. Gas fills the region between the mirrors (the slot in the spacer). A laser passes through the cavity to measure its optical length, nL , where L is the physical length and n is the gas refractive index. The intensity transmitted through the cavity is large when the laser wavelength is in resonance with the cavity, which occurs when the round-trip distance travelled by the light ($2L$) is an integer number (m) of wavelengths in the gas:

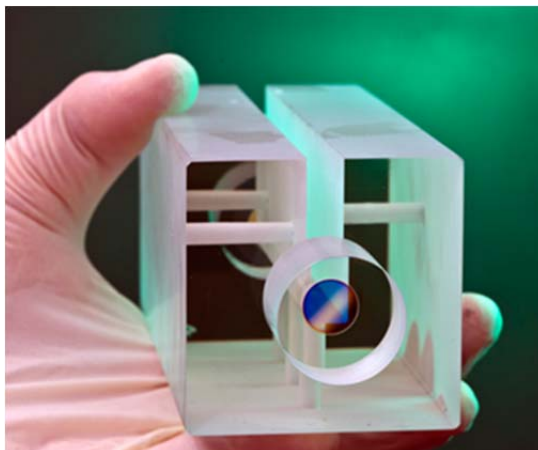


Figure 1. A Fabry-Perot cavity.

$$2L = m\lambda_{\text{gas}} \quad (1)$$

where the wavelength in gas (λ_{gas}) is related to wavelength in vacuum (λ_{vac}) according to

$$\lambda_{\text{gas}} = \lambda_{\text{vac}}/n. \quad (2)$$

(Equation (1) ignores several small but important effects such as mirror phase shifts and Gouy phase shifts [1].) The laser frequency (or equivalently, vacuum wavelength λ_{vac}) is servo-controlled to keep the laser in resonance with the cavity. If the physical length of the cavity is fixed, then a change in refractive index would tend to change λ_{gas} , but the servo system will re-adjust the laser frequency (thus changing λ_{vac}) so as to keep λ_{gas} constant and maintain resonance. The frequency change can then be measured to determine the change in refractive index. In principle, we could track this change as we go from vacuum (with known index $n=1$) to ambient pressure, and this would allow us to determine the refractive index. Equivalently, we

can think of this as measuring the change in the optical length of the cavity when gas is admitted: if the length is L at vacuum, nL' when gas is added, and if we assume that $L=L'$, the difference in optical length, $(n-1)L$, provides a measure of the gas refractivity $(n-1)$. The refractivity is in first approximation proportional to gas density or, equivalently, P/T , and thus can provide an indirect measure of pressure or temperature. (The proportionality is not exact: non-linearities such as non-ideal gas behavior must also be taken into account.)

A pressure measurement system now under construction contains two cavities within one block of glass, where one of the cavities is a vacuum reference and the second, similar to Fig. 1, is open to its surroundings. We will measure the frequency difference (beat frequency) between a laser locked to the vacuum reference and a second laser locked to the open cavity. A change in the beat frequency provides a measure of the change in gas refractive index, which can be

interpreted as a change in the gas pressure in the open cavity. For low pressures, the expected noise floor might be estimated from measurements we have carried out comparing the cavity of Fig. 1 to a separate cavity, both under vacuum. Some results are shown Fig. 2. With 10-s averages of the beat frequency, short-term noise is much smaller than long-term drift; the useful

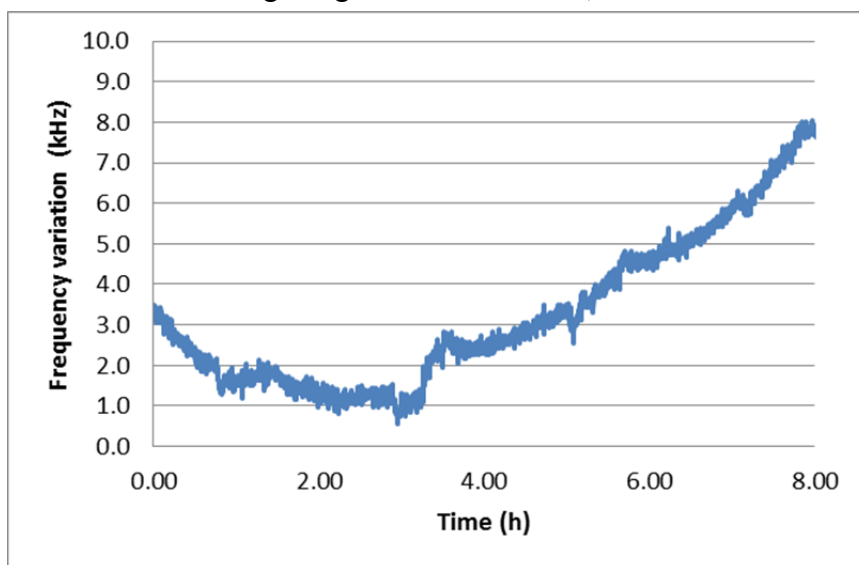


Figure 2. Drift in the frequency difference between two cavities. Uncertainties in the actual frequency measurement are too small to be visible on the graph.

precision is determined by the rate of drift and by how long is required to do a measurement after “zeroing” the device at vacuum. Typical drift rates shown in Fig. 2 are about 1 kHz/h; if the time for a measurement is under 1 hour, the useful resolution is then about 1 kHz. The amount of time that is required to perform a measurement depends on the time required to re-establish thermal equilibrium after adding gas, and can be quite long unless careful consideration is given to thermal management. Even at 1 h, the expected 1 kHz frequency variations correspond to a change in optical length of only 0.3 pm, demonstrating the high level of precision achievable. In terms of pressure measurement, the 0.3 pm change would correspond to a nitrogen pressure change of about 1 mPa. We would expect that our new device, where the two cavities share the same block of glass and have higher finesse, should substantially reduce noise and drift and should correspondingly improve the low-pressure resolution limit.

This example illustrates how fixed-length cavities provide a relatively straightforward path to sub-picometer precision. For measurements below 100 Pa, this precision is the limiting factor on accuracy, but at higher pressures systematic effects come into play. The analysis above assumed that the physical cavity length remained constant as the gas pressure changed, but this is not quite true due to the bulk modulus of the material. Corrections can be made to account for bulk modulus but the correction procedure is not sufficiently accurate to reach our goals.

A second, more complicated approach is needed to overcome this problem, employing a variable length optical cavity (VLOC). A pressure measurement system based on fixed length optical cavities (FLOC) has a good promise as a transportable standard, but can only reach its full potential after developing a second standard as described in the next section.

3. A Variable Length Cavity (VLOC) filled with helium. As explained previously, with a fixed length cavity we would like to measure the difference between the cavity length L in vacuum and the apparent length (optical length) given by nL when gas is present, and thus determine refractivity ($n-1$). The difficulty of this approach lies in the fact that the physical length L is not constant as pressure changes. This problem might be circumvented by working at constant pressure and generating two identical displacements L in variable-length Fabry-Perot cavities, one in gas and one in vacuum. The apparent displacement in the gas interferometer will be nL , and the difference between the two displacement measurements, $(n-1)L$, measures refractivity ($n-1$) and thus determines P/T . To achieve relative uncertainties of 1 part in 10^6 or better, it will be necessary to measure $(n-1)L$ to this accuracy. A gas of particular interest is helium, because the refractive index as a function of P and T can be calculated from first principles with high accuracy, so the refractive index measurement can be used to determine P absolutely (if T is known). For helium at atmospheric pressure, $n-1$ is 3×10^{-5} , and the difference in lengths $(n-1)L$ is $4.5 \mu\text{m}$. As this must be measured to better than 1 part in 10^6 , it will be necessary to measure the difference in displacements to better than 4.5 pm . (It is also necessary to measure L to better than 1 part in 10^6 , but this is not at all difficult.)

Our initial goal is to do the measurement with 3 pm standard uncertainty. (All uncertainty estimates in this paper are to be interpreted as standard uncertainty, coverage factor $k=1$.) It has already been mentioned that it is not too difficult to achieve sub-picometer precision when comparing two optical cavities. The effective length of an optical cavity can be measured with almost unlimited precision (even accuracy). The difficulty lies in relating the ultra-high accuracy of the internal cavity metrology to the actual measurand of interest. In the context of the VLOC, the problem is one of generating and measuring absolutely identical displacements in two optical cavities.

One scheme for achieving this goal is shown very schematically in the Fig. 3. As depicted, this scheme employs four Fabry-Perot interferometers, three in vacuum and one in gas. In principle the measurement requires only one of the vacuum interferometers, but at least one additional interferometer is needed to avoid a large Abbe offset, and the final interferometer completes a

system for monitoring angular variations (with nanoradian precision) when the moving mirror assembly is displaced. A sliding seal or bellows (not shown) allows for one baseplate to move, changing the length of the helium path (center) and vacuum paths (on the outside).

All of the moving mirrors must be rigidly mounted to the common baseplate so that their relative position in space remains stable at the picometer level during a displacement.

This can be achieved if the mirror substrates are made from ultra- low expansion glass (or ceramic) and the mirrors are rigidly attached to a plate of the same material by optical contact or similar stable bonding methods.

4. Comparing displacements at the picometer level. How can we achieve picometer accuracy in the measurement? The issues that need to be addressed include some familiar topics for those who do precision measurements -- Abbe offset, stage motion errors (pitch, yaw, straightness, etc.), interferometer misalignment, uncertainty of the basic length metric (laser vacuum wavelength), deadpath errors, geometric stability of the system, and imperfect surface form of the interferometer mirrors in combination with beam spread and beam walk. (“Beam walk” includes a variety of effects causing the beam to move across the surface of the mirrors as the moving baseplate is displaced). Another potential error source familiar when doing high precision interferometry-- fringe interpolation errors in a Michelson interferometer-- is here replaced by an analogous error of finding the center frequency of the Fabry-Perot resonance.

4.1 Abbe Error: Abbe offset, pitch, and yaw. One of the most important sources of error in any measurement is Abbe error, and the requirements for picometer measurements are extreme. Abbe error is θd where d is the Abbe offset and θ is a small angular variation due to pitch and yaw of the stage that moves the baseplate. (Small-angle approximations will be used throughout this paper.) For the apparatus shown in Fig. 3, the Abbe offset would be zero if the central interferometer mode is accurately located at the geometric center of the outer three interferometer modes. For illustration, a picture of a simplified planar system with just 3

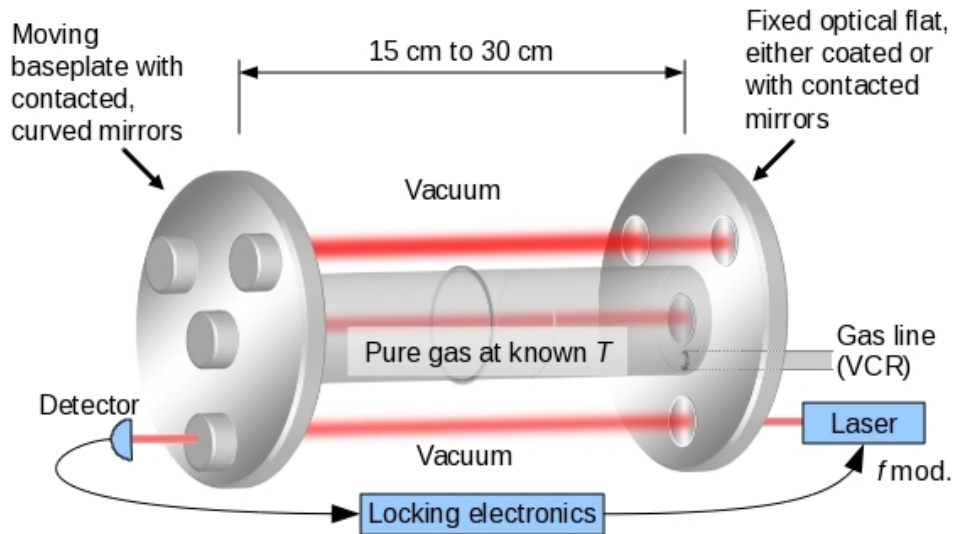


Figure 3. Conceptual picture of a variable-length cavity scheme, showing a laser locked to one of the four Fabry-Perot cavities.

interferometers (and no tube around the central interferometer) is shown in Figs. 4a and 4b. Figure 4a shows the initial position of the mirrors and Abbe offset d . In Fig. 4b, the baseplate with the curved mirrors has been moved to the left, accompanied by a pitch error θ . The difference between the average displacement of the two outer interferometers and the displacement of the central interferometer is then θd .

If the fixed base plate has flat mirrors that are accurately parallel, and the moving base plate has concave mirrors, the position of the modes is determined by the placement of the concave mirrors—more precisely, by the location of the centers of curvature of the mirrors. We should be able to determine the relative locations of the centers of curvature with the help of a high-accuracy coordinate measuring machine. If all mirrors but one are bonded to the baseplate, the proper location of the final mirror to minimize Abbe offset can be determined. Using a jig to set this location, it should be possible to bond the final mirror very near to the proper position. A realistic goal that can be achieved with good confidence is to demand that the Abbe offset d be kept below 0.1 mm.

In order to achieve our uncertainty goals, we hope to keep Abbe error at 1 pm or below. With an Abbe offset that could be as large as 0.1 mm, this will require that pitch and yaw errors are less than $0.01 \mu\text{rad}$ (0.002 arcsec). Such tiny angular errors will require the use of a fine tip/tilt control stage to correct errors in the coarse motion stage. (Rather than using fine adjustment to keep motion errors below $0.01 \mu\text{rad}$, it would suffice to numerically correct for Abbe error if the Abbe offset and angular errors can be measured with suitable accuracy, but it would be difficult to do this with sufficient accuracy to entirely circumvent the need for fine adjustment. Without fine adjustment, Abbe errors would also be accompanied by errors associated with beam walk, as described later.) One might think that angle measurements requiring $0.01 \mu\text{rad}$ uncertainty are rather demanding, but in the context of the VLOC this is not so. This angle corresponds to an imbalance in the outer three interferometers of 1 nm, which should be trivial compared to the picometer accuracy required in our displacement measurements. It also helps that the measurement is performed in vacuum and

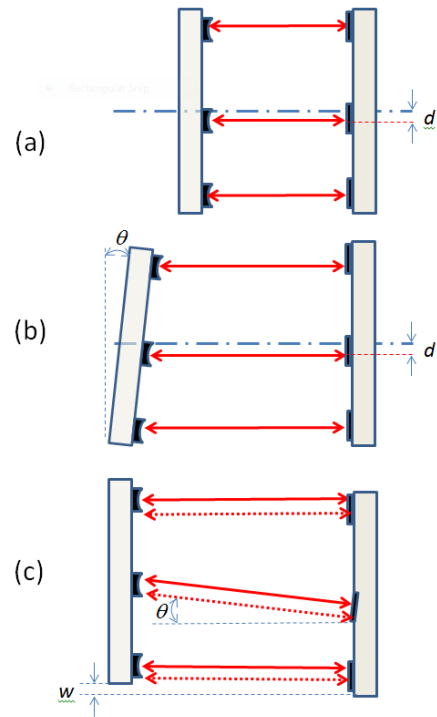


Figure 4. Two types of errors in a simplified system (three interferometers in a plane). The interferometer modes are shown as double-headed arrows. (a) The center line of the outer two interferometers, shown as dash-dot line, has Abbe offset d relative to the mode of central interferometer. (b) Cavity length is increased by moving the left baseplate, accompanied by pitch error θ . (c) (For Sec. 4.6.) Central mode is misaligned by angle θ relative to the outer modes (both before and after displacement); displacement is accompanied by straightness error w which causes the modes to move from position of dashed arrows to position of solid arrows.

that only a very small measurement range is required, as the angle will always be kept near zero by the fine adjustment stage.

4.2 Alignment error: If the four flat mirrors were simply four coated areas on a perfectly flat plate, the interferometer axes would be perfectly parallel. However, no plate is perfectly flat, and we cannot add individual angular adjustment to the four mirrors without compromising stability. We will require that the mirrors be parallel to within $1 \mu\text{rad}$ (0.2 arcsec)—a difficult but achievable specification.

4.3 Classic Cosine Error: There are several forms of alignment errors, referred to as “cosine errors” that can be associated with a measurement. The one that is most directly relevant here is a misalignment between the inner and outer interferometers, causing them to measure distances differing by $(1/2)\theta^2 L$ where, for the VLOC, L is the displacement and θ is the $1 \mu\text{rad}$ misalignment discussed above. This error is negligible for the VLOC.

4.4 Generalized Straightness error: For some purposes, it may be convenient to group three types of stage motion errors together as a “generalized straightness error.” Normal straightness errors, misalignment of the motion direction with the axis of the interferometer, and stage roll errors all have the effect of creating a translation of the moving mirrors perpendicular to the interferometer axis. For example, a misalignment of the motion axis with the axis of an interferometer by a small angle θ will cause the mirrors to translate perpendicular to the direction of motion by $L\theta$, where L is the displacement. This is equivalent in effect to a straightness error $L\theta$. Similarly, when the outside mirrors are located at radius r from the center of the plate, a roll about the center with magnitude θ_R causes the mirrors to translate by $r\theta_R$. Although this is not equivalent to a normal straightness error in the sense that the directions of the translations are different for each mirror, the effect is again to translate the mirrors perpendicular to the interferometer axis. For $r=2 \text{ cm}$ and $\theta_R=20 \mu\text{rad}$, the error would be $0.4 \mu\text{m}$, small enough that it would not be necessary to correct it. It would be desirable to have a stage with less than $20 \mu\text{rad}$ of roll, so that this goal can be reached without requiring additional fine adjustment of roll. Other generalized straightness errors can then be corrected by two fine translation stages.

4.5 Beam Walk: “Beam walk” is motion of the beam across the surface of the mirrors. It is a function of pitch, yaw, roll, straightness, and alignment with the motion direction. In reality, beam walk due to pitch and yaw errors become irrelevant once pitch and yaw are reduced to a suitable level so as to avoid Abbe errors; under these conditions, it depends only on the generalized straightness.

The position of the interferometer modes is fixed by the position of the concave mirrors. If the concave mirrors are on the moving element, the mode positions follow the mirror motion and are displaced according to the generalized straightness error. One way to measure the generalized straightness error is to observe the beam walk with a quadrant detector. It should be possible to

use this technique to measure the generalized straightness error and correct it, using fine motion stages, so that any residual beam walk is less than 1 μm .

As mentioned above, as a practical matter pitch and yaw errors do not cause significant beam walk because they must be corrected to such high accuracy for purposes of eliminating Abbe error. But for completeness it is worth noting that in the presence of a pitch or yaw error, the beam would walk by an amount $R\theta$ where θ is a pitch or yaw error and R is the mirror radius of curvature (about 0.5 m). This differs from the generalized straightness errors in that the beam position does not remain fixed relative to the concave mirrors; rather, it translates by $R\theta$ relative to the surface of *both* the concave and flat mirrors. The additional error due to motion of the beam across the surface of the concave mirrors is expected to be small.

4.6 Length errors associated with beam walk: As the interferometer beams walk, they move across the surface of the flat mirrors. The primary error that results from this motion is a combination of beam walk with the relative alignment error discussed previously. One way to think about the problem is to imagine what happens if the flat mirror (and mode axis) of the central interferometer is tilted by θ relative to the angle of the exterior interferometers, and that a straightness error causes the beams of all the interferometers to be displaced in a direction perpendicular to the axes of the outer interferometers. (See Fig. 4c.) Under these circumstances there is no change in the readings of the outer interferometers, but the displacement w has a small component along the direction of the axis of the central interferometer, causing its reading to change by $w\theta$. With our previous assumptions that $w \leq 1 \mu\text{m}$ and $\theta \leq 1 \mu\text{rad}$, the resulting error would be $\leq 1 \text{ pm}$.

Note: more precisely, θ is the difference between the slope of the inner interferometer flat mirror surface and the average slope of the outer interferometer mirror surfaces, where all slopes are measured along the direction of the beam walk.

We will monitor the beam walk directly and use fine control to eliminate all these sources of beam walk except for roll. Under these circumstances, the only unavoidable errors are set by (a) our ability to measure straightness and (b) a roll-induced straightness error of 0.4 μm that we are not correcting. We can probably measure straightness within 1 μm without much difficulty. If necessary, the straightness measurement could be done much better at the expense of added complexity.

After correction with a fine adjustment stage, “beam walk” will then not exceed 1 μm , and the beam-walk/alignment error should not exceed 1 pm.

4.7 Surface figure: The form of the mirror surfaces affects the shape of the interferometer mode and changes fine details of how phase evolves as a function of distance. In addition, the local slope of the flat mirror surface determines the overall direction of the mode and thus plays a role in determining the alignment error discussed previously. Variations in local slope away from the

ideal might be considered to be the lowest-order effect of imperfect surface figure; variations on the order of 1 μ rad can be expected even for the best surfaces available. Here we discuss possible higher-order effects. The next effect to consider is local curvature of both the concave and nominally flat surfaces, including the possibility that the curvature might differ along two axes, corresponding to astigmatism. These effects give rise to Gouy phase shifts (diffraction effects). Durand et al. [2] have shown that it is possible to measure the local curvature/astigmatism of the two surfaces and to make corrections for the Gouy shift at the sub-picometer level.

Beyond curvature, the imperfect mirror surfaces have topological features on a variety of length scales that may be hundreds of picometers high (even for a super-polished mirror). At some level these features will perturb the mode structure and give rise to phase shifts analogous to the Gouy shift. Perhaps more important might be the fact that, if the beam walks across the mirror surface, this could give rise to errors at the picometer level simply because the average surface height will change as the beam samples different positions on the imperfect surface. The same kinds of errors can also occur because the mode diameter (beam diameter) changes as the distance between the two interferometer mirrors changes. However, all of these higher-order effects appear to be likely irrelevant; the experiment [2] suggests that it suffices to make the Gouy corrections for astigmatic surfaces and additional corrections are required only at the sub-picometer level. Based on those results, we estimate that possible errors are below 0.6 pm.

In reality, our experiment could yield a correct value for the refractive index even if we ignored the Gouy phase shifts. First of all, the Gouy corrections mostly cancel if all the mirrors have nominally the same curvature. Furthermore, the residual errors could be corrected by measuring and subtracting the apparent refractivity at zero pressure. (The curvature of the mirrors will not change noticeably due to pressure distortions.)

4.8 Geometric Stability: The geometry of the flat plates that hold the mirrors must remain fixed during the displacement, so as to guarantee that the average displacement of the outer interferometers is equal to the displacement of the inner interferometer at the picometer level.

To perform a displacement it is necessary to include a sliding seal or a bellows in the central pipe shown in Fig. 3. Friction in the seal or extension/compression of the bellows will apply forces to the end plates. Finite element calculations suggest that it is not trivial to avoid the resulting distortions, but with careful design it should be possible to completely decouple these forces from the end plates.

A second problem is possible helium diffusion into the glass of the baseplate or mirror substrates. With our existing cavities (Fig. 1), which use a titania silicate low expansion glass, we have observed that helium infusion causes the length to change fractionally by $\Delta L/L = 7 \times 10^{-10}$ per hour, and this rate of change was constant during 10 hours of observation. For a 1 cm thick mirror substrate contacted to the end plate, the expected drift is then 6 pm/h, and the importance

of this drift depends critically on how much time will be required to do a measurement. Over a period of 30 min, the drift is only 3 pm, and the effect can be mostly eliminated by measuring first at the initial position, followed by a 15 cm displacement to the final position and a return to the initial position for a final measurement. Assuming the drift is linear in time, averaging the two readings at the initial position would effectively eliminate it.

However, there is some danger that making displacements will disrupt the thermal environment, in which case it may require many hours to re-establish thermal equilibrium. In that case, eliminating the drift assuming a linear time variation would become much more problematic. This problem might be entirely avoided (with some tradeoffs) by using a material for the baseplates and mirror substrates that is not permeable to helium.

The geometry is not sensitive to uniform thermal expansion, but in principle could be affected by thermal gradients that are a function of position of the moving plate. If the mirror substrate of the internal interferometer expanded relative to the external interferometers by 1 pm, this will cause a 1 pm error in our result. However, any such error should be much less than 1 pm for the VLOC, with gradients less than 0.2 mK, mirror substrates ≈ 1 cm thick, and the thermal expansion coefficient $\leq 3 \times 10^{-8}/C$. A thermal gradient across the base plate could also cause it to bend, but the expected effect is again negligibly small.

Material aging might also cause instability of the geometry. A uniform change in dimensions would be balanced, but one might imagine that relieving of stresses could cause the plate to warp over time. However, optical cavities such as our FLOC have generally demonstrated good long term stability. Observed changes in length have been less than 3 pm/d, where the change includes both uniform aging of the bulk material plus any possible warping of the end plates (mirror substrates) and aging of the mirror coatings. The effects of warping could be somewhat worse for the VLOC with its relatively large base plate, but it seems unlikely that warping could exceed a few picometers over a run, and can be largely eliminated by averaging readings at the start and end of a run, as was discussed for helium absorption.

4.9 Locking accuracy: As discussed for the case of a fixed-length cavity, this is a sub-picometer error. The main problem to be aware of is unintended amplitude modulation of the laser beam, which can vary with time and shifts the apparent center frequency of the cavity transmission maximum.

4.10 Length Metric: The basic metric is the laser vacuum wavelength. Errors in the metric would be precisely common mode except for the fact that the change in optical pathlength in the middle interferometer is larger than the displacement of the outer interferometer because of the refractive index of helium. The difference is only about 5 μm . If we know the laser wavelength to 1 part in 10^7 , the resulting error is then 0.5 pm. This is trivially achieved if a helium-neon laser is employed for the interferometer and its wavelength is measured by comparison to any commercial frequency-stabilized reference laser.

The requirements on laser frequency would be much more demanding if the comparison of the vacuum and gas paths was carried out using a back-to-back geometry. With differences in path length exceeding 0.1 m, picometer accuracy would require frequency metrology at the 10^{-11} level, a significant complication.

4.11 Deadpath: As the gas density (primarily pressure) changes, the optical length changes. This has no real effect if the measurement begins at zero pathlength, but when it begins at non-zero pathlength, the pressure change effectively represents a change in the initial position of the measurement, which will give an error unless it is measured and corrected. A high-quality piston gage may suffice to keep the pressure constant during a run, but it is challenging: if the deadpath is 15 cm (equal to our displacement), then a fraction change in helium density of 5×10^{-7} will cause a shift in zero position of 2.7 pm. Once again, this effect can be largely eliminated if the pressure drift is linear in time and measurements at the initial position are averaged before and after the displacement. Also, it should be possible to measure and correct for pressure changes if the measuring device is suitably stable; one possibility is a FLOC as discussed previously.

4.12 Summary of errors, repeatability of errors with multiple runs: An important question is, what errors are systematically repeatable, which vary in a predictable manner vs time, and which are just noise? Consider, for example, the largest potential errors that were discussed above. If we simply do a single two-point displacement measurement, without a return to the initial position, errors could be as large as:

- (1) Geometric instability will contribute at least 3 pm uncertainty due to helium infusion, more if the measurement requires long times to reach thermal equilibrium.
- (2) Deadpath error could be as large as 2.7 pm if pressure is unstable at the level of 0.5×10^{-6} and the instability cannot be measured and corrected.
- (3) Abbe errors are expected to be about 1 pm at any position, or 1.4 pm when measuring a two-point displacement.
- (4) Beam walk combined with alignment errors will contribute about 1 pm uncertainty.
- (5) A combination of beam spread and imperfect surface figure can contribute an estimated 0.6 pm of uncertainty.
- (6) Other errors are small in comparison and add very little to the total uncertainty.

Adding these uncertainties in quadrature gives a projected combined standard uncertainty of 4.5 pm, not quite as good as what we hope to achieve. But all of these errors can be reduced in one manner or another. If they are random in nature, they can simply be reduced by averaging multiple measurement runs. This would include Abbe errors, which will not repeat run-to-run because the angular errors are always re-adjusted to nominal zero. At the opposite extreme, if errors are totally repeatable including independent of pressure (such as beam spread), they can be

corrected on the basis of measurements at zero pressure. If they are neither totally repeatable nor random, but vary approximately linearly in time (geometry instability from helium infusion, deadpath error due to drift in a piston gage) they can be greatly reduced by returning to the original position and averaging (a drift-eliminating experimental design). Finally, “beam walk” errors will have a random component, which can be reduced by averaging, but may also have a systematic component due to systematic errors in straightness measurement. The systematic part will repeat at zero pressure and can be eliminated in the same manner as the “beam spread” error.

It can probably then be argued that most of the major sources of error will be reduced by at least a factor of 2 with averaging two pairs of out-and-back runs in a drift-eliminating design. This will bring us to our goal of < 3 pm overall uncertainty.

5. Conclusion. Sub-picometer precision can be straightforward in a mechanically simple system such as our fixed length cavity (FLOC). But achieving useful measurements relating to the external world at the picometer level is much more difficult, as evidenced by the VLOC where multiple lasers and fine control motion stages are required. In this article we have outlined a path toward achieving useful picometer-level measurements, where measurements in independent interferometers must be related to each other in a non-trivial manner. Success in actually achieving this result is not guaranteed. For example, we have relied on an assumption that dimensional instability due to helium absorption can be overcome either by making measurements on a fairly fast time scale (requiring very careful thermal management) or by employing non-permeable materials for the base plate (materials with which we have less experience and have some reservations regarding overall performance). We nevertheless have outlined a plausible road map for reaching the desired goal. Significantly different alternative approaches are also under consideration. The variable length cavities could be replaced by a variable length cell, where the pathlength through gas in the cell might be compared to pathlength in surrounding vacuum using an interferometer with a geometry as described by Weichert et al [3,4]. At the present time, drifts in this type of interferometer [4] would make it difficult to achieve our target accuracy, but the technology is still under development and may be expected to improve. A cell-based approach could reduce the complexity of a variable-length system.

Systems designed around fixed-length cavities (or possibly fixed-length vacuum cells) can serve as excellent transportable measurement systems, and the potential errors of these systems can be characterized using the “gold standard” variable length approach. For pressure measurement, the transportable systems will use nitrogen as the working medium, and the VLOC will be instrumental in high-precision measurements of the relationship between nitrogen refractive index and pressure.

References.

- [1.] P. Egan and J. Stone, “Absolute refractometry of dry gas to ± 3 parts in 10^9 ”, *Appl. Opt.*, **50**, pp. 3076 – 3086, 2011.
- [2] M. Durand, Y. Wang, and J. Lawall, “Accurate Gouy phase measurement in an astigmatic optical cavity”, *Appl. Phys. B*, **108**, pp. 749–753, 2012.
- [3] C. Weichert, P. Köchert, R. Köning, J. Flügge, B. Andreas, U. Kuetgens, and A. Yacoot, “A heterodyne interferometer with periodic nonlinearities smaller than ± 10 pm”, *Meas. Sci. Technol.* **23**, 094005 (7pp), 2012.
- [4] C. Weichert, J. Flügge, P. Köchert, R. Köning, and R. Tutsch “Stability of a fiber-fed heterodyne interferometer” 10th IMEKO Symp. Laser Metrology for Precision Measurement and Inspection in Industry (Düsseldorf: VDI) pp. 243–50, 2011.